The Journal of Experimental Medicine

Neutrophil mobilization via plerixafor-mediated CXCR4 inhibition arises from lung demargination and blockade of neutrophil homing to the bone marrow

Sapna Devi,[1] Yilin Wang,[1] Weng Keong Chew,[1] Ronald Lima,[2] Noelia A-González,[3] Citra N.Z. Mattar,[4] Shu Zhen Chong,[1] Andreas Schlitzer,[1] Nadja Bakocevic,[1] Samantha Chew,[1] Jo L. Keeble,[1] Chi Ching Goh,[1] Jackson L.Y. Li,[1] Maximilien Evrard,[1] Benoit Malleret,[1] Anis Larbi,[1] Laurent Renia,[1] Muzlifah Haniffa,[1,5] Suet Mien Tan,[6] Jerry K.Y. Chan,[4,7,8] Karl Balabanian,[9] Takashi Nagasawa,[10,11] Françoise Bachelerie,[9] Andrés Hidalgo,[3] Florent Ginhoux,[1] Paul Kubes,[2] and Lai Guan Ng[1]

[1]Singapore Immunology Network (SIgN), A*STAR (Agency for Science, Technology and Research), Biopolis, 138648 Singapore
[2]Calvin, Phoebe, and Joan Snyder Institute for Infection, Immunity, and Inflammation, University of Calgary, Alberta T2N 1N4, Canada
[3]Department of Epidemiology, Atherothrombosis and Imaging, Fundación Centro Nacional de Investigaciones Cardiovasculares (CNIC), 28029 Madrid, Spain
[4]Experimental Fetal Medicine Group, Yong Loo Lin School of Medicine, National University of Singapore, 119228 Singapore
[5]Institute of Cellular Medicine, Newcastle University, Newcastle upon Tyne NE2 4HH, England, UK
[6]School of Biological Sciences, Nanyang Technological University, 637551 Singapore
[7]Department of Reproductive Medicine, KK Women's and Children's Hospital, 229899 Singapore
[8]Cancer and Stem Cell Biology Program, Duke-NUS Graduate Medical School, 169857 Singapore
[9]Inserm Unite Mixte de Recherche (UMR) S996, Universiteï Paris-Sud, Laboratory of Excellence in Research on Medication and Innovative Therapeutics, 92140 Clamart, France
[10]Department of Immunobiology and Hematology, Institute for Frontier Medical Sciences, Kyoto University, Kyoto 606-8507, Japan
[11]Japan Science and Technology Agency (JST), Core Research for Evolutional Science and Technology (CREST), Tokyo 102-0076, Japan

Blood neutrophil homeostasis is essential for successful host defense against invading pathogens. Circulating neutrophil counts are positively regulated by CXCR2 signaling and negatively regulated by the CXCR4–CXCL12 axis. In particular, G–CSF, a known CXCR2 signaler, and plerixafor, a CXCR4 antagonist, have both been shown to correct neutropenia in human patients. G–CSF directly induces neutrophil mobilization from the bone marrow (BM) into the blood, but the mechanisms underlying plerixafor–induced neutrophilia remain poorly defined. Using a combination of intravital multiphoton microscopy, genetically modified mice and novel in vivo homing assays, we demonstrate that G–CSF and plerixafor work through distinct mechanisms. In contrast to G–CSF, CXCR4 inhibition via plerixafor does not result in neutrophil mobilization from the BM. Instead, plerixafor augments the frequency of circulating neutrophils through their release from the marginated pool present in the lung, while simultaneously preventing neutrophil return to the BM. Our study demonstrates for the first time that drastic changes in blood neutrophils can originate from alternative reservoirs other than the BM, while implicating a role for CXCR4–CXCL12 interactions in regulating lung neutrophil margination. Collectively, our data provides valuable insights into the fundamental regulation of neutrophil homeostasis, which may lead to the development of improved treatment regimens for neutropenic patients.

Neutrophils are produced and stored in the BM, and the control of neutrophil release from BM critically regulates the circulating numbers of these cells in blood. Low numbers of circulating neutrophils (neutropenia) can lead to chronic or even life threatening infections

S. Devi, Y. Wang, and W.K. Chew contributed equally to this paper.

in human patients if left untreated. Although neutropenia can result from a wide range of underlying causes, including pathogen exposure, pharmacological insults, and genetic factors, the therapeutic options for neutropenic patients are limited.

Numerous studies have shown that CXCR2 and CXCR4 expressed by neutrophils play crucial roles in maintaining neutrophil homeostasis (Semerad et al., 2002; Martin et al., 2003; Suratt et al., 2004; Wengner et al., 2008; Eash et al., 2010; Köhler et al., 2011b). CXCR2 is important for the mobilization of neutrophils from the BM (Suratt et al., 2004; Eash et al., 2010; Köhler et al., 2011b; Mei et al., 2012), whereas CXCR4 promotes neutrophil retention in the BM via interactions with CXCL12 expressed by BM stromal cells (Shirozu et al., 1995; Ponomaryov et al., 2000; Eash et al., 2010). Accordingly, current treatments for neutropenic patients are predominantly directed toward correcting the neutrophil deficiency by mobilizing neutrophils to the circulation while also attempting to treat/control the underlying infection. Granulocyte-CSF (G-CSF) is widely used to treat neutropenic patients in the clinic (Ulich et al., 1988; Lieschke and Burgess, 1992a,b), and previous studies have demonstrated that G-CSF–induced neutrophil mobilization is dependent on CXCR2 signaling (Eash et al., 2010; Köhler et al., 2011b). In contrast, transient blockade of CXCR4 signaling using a small molecule antagonist of CXCR4, plerixafor (AMD 3100), has also been shown to induce neutrophilia (Martin et al., 2003). Inhibition of CXCR4 signaling by plerixafor was effective in correcting neutropenia in a mouse model (Balabanian et al., 2012) and in human patients (Dale et al., 2011; McDermott et al., 2011) with gain-of-function mutations in CXCR4 that confers the warts, hypogammaglobulinemia, immunodeficiency, and myelokathexis (WHIM) syndrome (Hernandez et al., 2003). This, therefore, provides in vivo evidence to show that CXCR4 inhibition can be a new and effective treatment for neutropenic patients.

The dynamic regulation of circulating neutrophil numbers depends on a complex and dynamic interplay between various cellular and molecular components in multiple different tissue compartments, and is thus difficult to dissect using conventional laboratory techniques. Due to the well documented role of CXCR4 in the retention of neutrophils and stem cells in the BM niche (Martin et al., 2003; Levesque et al., 2004; Eash et al., 2009), CXCR4 inhibition-induced neutrophilia is thought to result from increased neutrophil egress from the BM (Martin et al., 2003; Suratt et al., 2004; Eash et al., 2009, 2010), but this has not been demonstrated directly.

To overcome this challenge, we studied neutrophil mobilization using a dynamic and integrative physiological approach. We used the technique of intravital multiphoton microscopy to directly examine BM neutrophil activity, at the single-cell level, in response to G-CSF or CXCR4 inhibition by plerixafor treatments in vivo. Here, we provide direct evidence that G-CSF–induced neutrophilia results primarily from increased neutrophil motility and mobilization from the BM, whereas plerixafor had no detectable effects on neutrophil migratory activity in this compartment. Instead, we observed that plerixafor increased circulating neutrophil numbers by blocking neutrophil trafficking to the BM while promoting neutrophil release from the lung. In addition, we have also examined how the gain-of-function mutations in CXCR4 influence neutrophil mobilization and homing patterns in vivo. Together, these data define distinct mechanisms of neutrophil mobilization from different tissue compartments into the blood, which provide new insights into neutrophil homeostasis, and may lead to better treatment regimens for neutrophil-related diseases.

RESULTS

Blood neutrophil frequency is rapidly increased after G-CSF or plerixafor treatment

To investigate how G-CSF or CXCR4 inhibition by plerixafor may impact neutrophil activity in the BM, we first established an intravital imaging model that enabled the visualization of these cells within the BM microenvironment of the skull (calvarium; Mazo et al., 1998; Fig. 1 a). Our preliminary dynamic imaging studies showed that the majority of neutrophils in the BM of lysozyme (LysM)-GFP mice (Faust et al., 2000; Fig. S1) were relatively inactive under homeostatic conditions, and neutrophil egress from the BM was a rare event (not depicted). We then visualized steady-state neutrophil distribution relative to BM sinusoids by examining chimeric mice created from irradiated ubiquitous tomato fluorescent protein–expressing (mT/mG) mice (Muzumdar et al., 2007) that were reconstituted with LysM-GFP BM cells, such that their endothelial cells expressed red fluorescent protein and neutrophils expressed green fluorescent protein. Dynamic imaging of these mice confirmed that neutrophils in the marrow space exhibited low baseline motility (∼3 µm/min). However, we also observed that perisinusoidal neutrophils displayed an active probing behavior, and that a small fraction of these cells successfully transmigrated from the abluminal surface of the sinusoidal walls into circulation (Fig. 1 b; Video 1).

Having examined the neutrophil activities in the BM under steady-state conditions, we next sought to investigate the BM neutrophil response to promobilization signals by G-CSF and plerixafor treatments. We first determined the appropriate timing for imaging by quantifying the number of circulating neutrophils at various time points after G-CSF or plerixafor administration (Fig. 1 c). Consistent with previous studies, we observed that a single dose of s.c. injection of clinical grade G-CSF (Ulich et al., 1988; Semerad et al., 2002) or plerixafor (Martin et al., 2003) resulted in an increase in the number of circulating neutrophils. Blood neutrophil counts progressively increased over a 4-h period after G-CSF administration, whereas circulating neutrophil numbers peaked at 1–2 h and returned to near basal levels by 4 h after plerixafor treatment. These results suggest that observable changes of neutrophil behavior should occur in the BM within the first
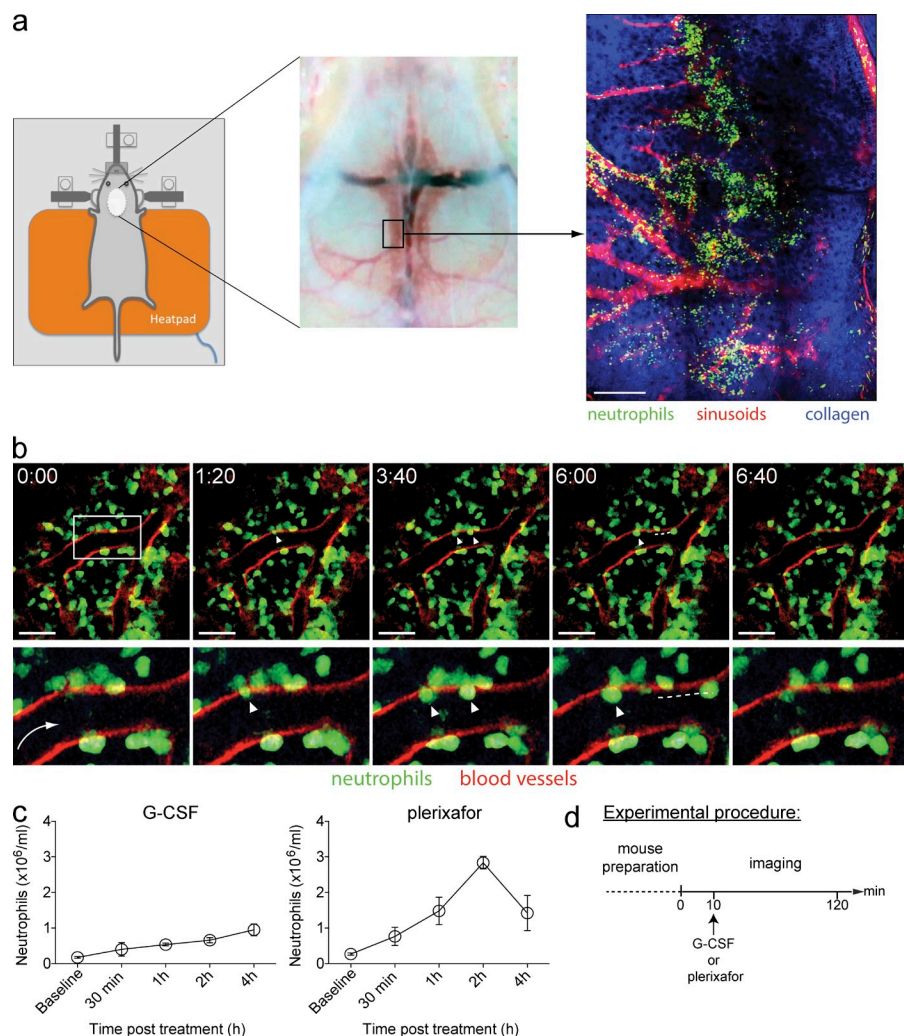
Figure 1. Intravital multiphoton microscopy of murine skull BM. (a) Schematic overview of the imaging region of mouse skull. (Left) Set-up of an anaesthetized mouse on a custom-made intravital imaging stage. (Middle) Removal of skin and exposure of the skull bone. (Right) A snapshot of the skull BM microenvironment in a LysM-GFP mouse, consisting of GFP+ neutrophils (green), sinusoids (vasculature labeled with TRITC dextran; red), and bone collagen matrix (second harmonic generation; blue). Bar, 200 µm. (b) Representative time-lapse images showing resting state neutrophil activity in skull BM in a chimeric mouse (LysM-GFP BM transferred into irradiated mT/mG mice; $n = 3$ mice). The white box specifies the region viewed at high magnification (bottom). The arrow indicates the direction of blood flow, and arrowheads indicate GFP+ neutrophils migrating through the sinusoidal endothelium (red), followed by their release into the circulation (white dashed line). Time scale (minutes:seconds) is shown above images. Bars, 40 µm. See also Video 1. (c) Kinetics of circulating neutrophil numbers in WT mice in response to a single s.c. injection of 250 µg/kg G-CSF or 5 mg/kg plerixafor treatment ($n = 4$ mice per group per time point). All data are shown as mean ± SEM. A representative set of data were shown from three independent experiments. (d) The experimental procedure for multiphoton imaging of the skull BM. This involved preparation of the mouse followed by 2 h of imaging, which involved 10 min of basal imaging and post–G-CSF or -plerixafor s.c. injection.

2 h after treatment. We therefore subsequently designed our experiments to image neutrophil responses in the BM from 0 to 2 h after treatment (Fig. 1 d).

BM neutrophil motility is enhanced by G-CSF

We next imaged the BM microenvironment in LysM-GFP mice, in which all myelomonocytic cells are tagged with GFP. Neutrophils, however, constitute the major population of these GFP-positive cells (>70%), and they exhibit the highest GFP expression (Fig. S1). Consequently, neutrophils can be easily distinguished from other myelomonocytic cell types based on their high GFP intensity (Chtanova et al., 2008; Peters et al., 2008; Kreisel et al., 2010; Ng et al., 2011; Li et al., 2012). In addition, the BM sinusoids were visualized by intravenous injection of TRITC-dextran (Fig. 2 a). Increased neutrophil motility was detected within ∼11 min after a single s.c. injection of G-CSF (mean = 10.63 min ± 0.31 SD, $n = 3$; Fig. 2 b). These data are in agreement with a previous study of G-CSF effects on neutrophil motility in tibial BM (Köhler et al., 2011b). In mice that received G-CSF, neutrophils were observed to migrate toward the sinusoids before exiting into the blood

circulation (Video 2). Our tracking analysis showed that neutrophils, at the whole population level, switched from a low motility phenotype (mean velocity, 3.28 µm/min; median velocity, 2.94 µm/min over a 5-min tracking period) under resting conditions to a high motility phenotype that peaked at ∼25 min after G-CSF injection (mean velocity, 6.51 µm/min; median velocity, 6.24 µm/min over a 5-min tracking period; Fig. 2 c) and gradually decreased thereafter, but cell migratory activity remained elevated for as long as 2 h after administration. Additionally, we devised a method to quantify endogenous neutrophil egress based on the relative green fluorescent intensity remaining in the marrow space. With this method, we observed a decrease of the green fluorescent intensity in the marrow space in G-CSF–treated mice, indicating neutrophils exiting the BM (Fig. 2 e). This response peaked at ∼40 min after G-CSF administration. It is also interesting to note that the GFP intensity recovered to basal levels at later time points after G-CSF treatment. Conceivably, this was a result of migrating neutrophils from other regions of the BM replenishing the depleted marrow space. Consistent with a previous study by Köhler et al. (2011b), we observed that G-CSF–induced
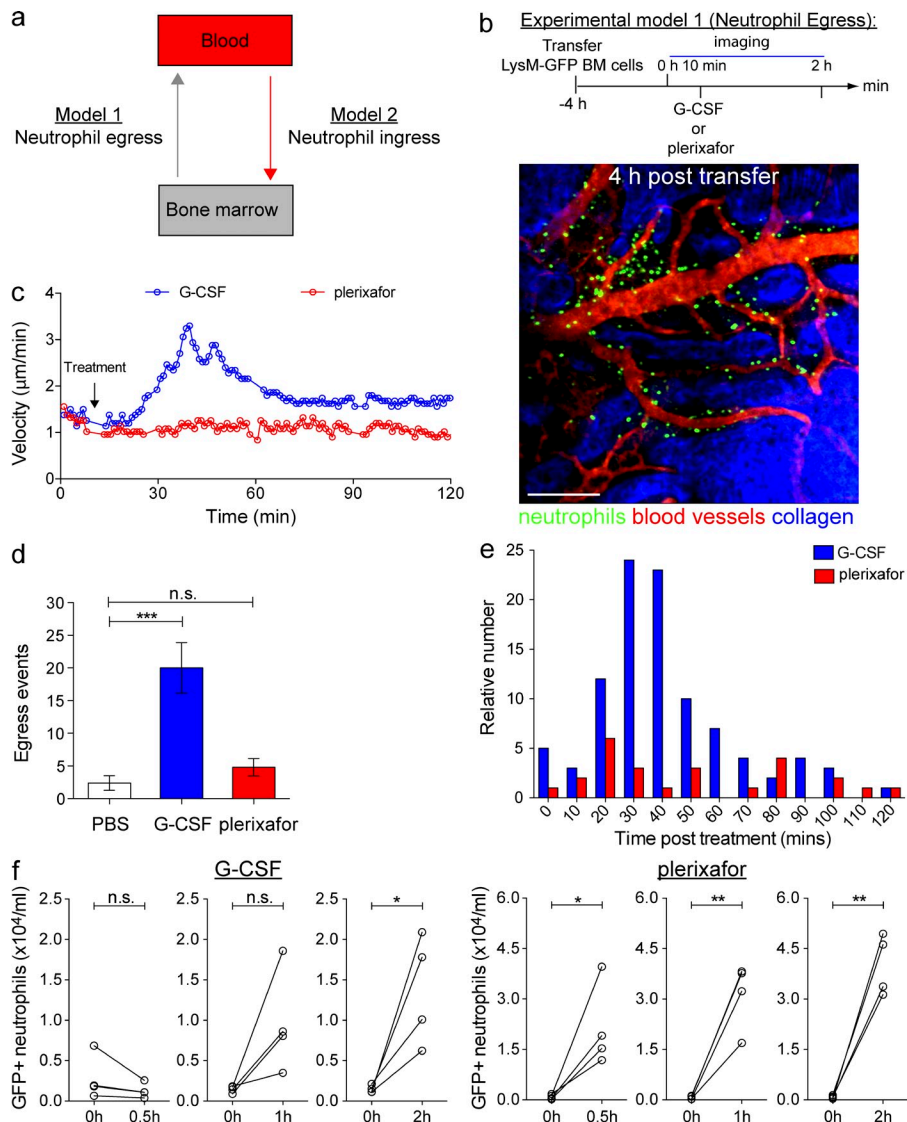
Figure 2. Neutrophil motility in skull BM is increased by G–CSF but not by plerixafor. (a) Snapshots of migrating neutrophils in the BM of LysM-GFP mice during resting state (top left), and 25 min after G-CSF injection (top right). White boxes and circles indicate the region of GFP+ neutrophil mobilization from the BM cavity toward the sinusoids (vasculature labeled with TRITC dextran; red). (Bottom) Same images as in the top, with the green signal (neutrophils) omitted. White lines indicate the tracks of migrating neutrophils over the 10-min imaging period. Bars, 40 µm. (b) Mean instantaneous velocity of migrating GFP+ neutrophils in skull BM in a LysM-GFP mouse both before and after G-CSF (representative of three independent experiments). (c) The mean migratory velocities (top) and the relative frequency distribution of neutrophil velocities (bottom) at different time points after G-CSF injection (5-min tracking period, n = 3 per group). Each symbol corresponds to an individual tracked neutrophil and the bars indicate the mean velocity during resting, 25 min and 50 min post-G-CSF injection. (d) Snapshots of neutrophils in BM during resting state (left) and after plerixafor treatment (5 mg/kg s.c.; right). White lines indicate the tracks of neutrophils over the 1-h tracking period after plerixafor injection (vasculature labeled with TRITC dextran, red). Bars, 40 µm. (e) Relative GFP fluorescence intensity in the skull BM parenchymal region in LysM-GFP mice treated with G-CSF or plerixafor over time (representative of three independent experiments). (f) Mean instantaneous velocity of migrating monocytes in the BM of CX_3CR1-GFP mouse after G-CSF treatment. Graph shows a representative dataset from three independent experiments. The arrow indicates the time point whereby G-CSF was administered s.c. (g, Top) Mean instantaneous velocity of migrating GFP+ neutrophils in skull BM in a LysM-GFP mouse at resting state and after plerixafor treatment (data from three independent experiments). (g, Middle) The mean migratory velocities of neutrophils at different time points after plerixafor injection (30-min tracking period, n = 3 per group). (g, Bottom) The relative frequency distribution of neutrophil velocities (dataset from a representative mouse). Each symbol corresponds to an individual tracked neutrophil and the bars indicate the mean velocity of the whole population. A Student's two-tailed unpaired t test was performed. Numbers above the frequency distributions indicate the median velocity of the population. PI = post-injection, n.s. = not significant. See also Video 2.

neutrophil motility is dependent on CXCR2 (unpublished data), and that the observed increase in cell motility after G-CSF treatment was restricted to neutrophils because BM monocyte migratory activity was not enhanced after G-CSF injection in CX_3CR1-GFP mice subjected to the same BM imaging protocol (Fig. 2 f).

Figure 3. Differential effects of G–CSF and plerixafor on neutrophil mobilization in vivo. (a) A schematic representation of the two models established to study neutrophil egress (from BM to blood) and neutrophil ingress (from blood to BM). (b, Top) Experimental model 1: BM cells from LysM-GFP mice were transferred into WT recipient mice at least 4 h before multiphoton imaging of the skull BM. Recipient mice were subsequently injected with PBS, G-CSF, or plerixafor s.c., followed by imaging for up to 2 h (n = 5 per group). (b, Bottom) A representative snapshot of the skull BM 4 h after cell transfer. GFP+ cells (green) were predominantly present in the BM cavity outside the sinusoids (labeled with TRITC dextran; red). Bar = 200 µm. (c) Mean instantaneous velocities of transferred GFP+ neutrophils in mice treated with G-CSF or plerixafor. Each graph shows a data-set from a representative mouse. (d) Mean GFP+ neutrophils egressed from the skull BM after PBS, G-CSF, or plerixafor treatment (n = 5 per treatment group). All data are shown as mean ± SEM. One-way ANOVA analysis was performed. (e) The frequency distribution of neutrophils egressed from the BM into the sinusoidal circulation at various time points after G-CSF or plerixafor injection. Analysis was performed on data pooled from five mice per treatment group. See also Videos 3–5. (f) The number of circulating GFP+ neutrophils before and after G-CSF (left) or plerixafor (right) treatment (n = 4 per group per time point). Each line corresponds to a single mouse and shows the number of circulating neutrophils at resting state and 2 h after G-CSF or plerixafor treatment. Student's two-tailed paired t test was performed. *, $P < 0.05$; **, $P < 0.01$; ***, $P < 0.001$; n.s. = not significant.

Neutrophilia induced by CXCR4 inhibition is independent of mobilization from the BM

Interactions between CXCR4 and CXCL12 promote neutrophil retention in the BM and contribute to neutrophil homeostasis (Martin et al., 2003; Suratt et al., 2004; Eash et al., 2010). Accordingly, inhibition of CXCR4 signaling by plerixafor is thought to induce peripheral neutrophilia by increasing neutrophil release from the BM (Martin et al., 2003; Broxmeyer et al., 2005). However, a recent study has suggested that plerixafor treatment can increase blood neutrophil frequency by mobilizing neutrophils from sites other than the BM (Balabanian et al., 2012). To assess whether CXCR4 inhibition–induced neutrophilia is derived from the BM, we first performed dynamic imaging experiments on BM in LysM-GFP mice after plerixafor administration. Contrary to our initial expectations, we observed no change in the migratory behavior of neutrophils after plerixafor treatment (Fig. 2 d). Neutrophils failed to migrate toward the sinusoids and no cells were observed to

exit from the BM during the entire imaging period (up to 2 h after drug administration, Fig. 2 e). Despite inducing profound blood neutrophilia, administration of plerixafor had no detectable effect on the migratory behavior of BM neutrophils (Fig. 2, e and g; Video 2). To exclude the possibility that these differential neutrophil responses to G-CSF and plerixafor were specific to the skull BM, we performed additional imaging experiments in tibial BM (Köhler et al., 2011a,b). Neutrophils in tibial BM displayed similar mobilization responses to their skull BM counterparts; G-CSF injection increased cell motility whereas plerixafor treatment did not (unpublished data). These data confirmed that neutrophil mobility in the skull BM displays similar characteristics to BM neutrophils at other sites. Based on these results, we therefore used the model of the skull BM for our subsequent imaging studies, as the skull BM set-up is more robust and less surgically invasive than the tibial model.

Thus, despite exerting different influences on BM neutrophil activity, both G-CSF and plerixafor were capable of

inducing marked increase in circulating neutrophil numbers (Fig. 1 c). To better define the mechanisms that account for this finding, we established two independent experimental models which examine how G-CSF and plerixafor treatment influenced neutrophil egress (BM to blood; experimental model 1) and neutrophil ingress (blood to BM; experimental model 2; Fig. 3 a). We used exogenously transferred GFP+ neutrophils to overcome the technical challenge of tracking endogenous BM neutrophils, as it is difficult to distinguish individual cells within the congested marrow space.

Neutrophil entry and exit from the BM are likely to contribute to the regulation of blood neutrophil counts (Løvås et al., 1996; Suratt et al., 2001; von Vietinghoff and Ley, 2008). Thus, we sought to correlate the rate of neutrophil exit from the BM with the neutrophil frequency in blood. In the egress model, freshly isolated LysM-GFP+ BM cells were adoptively transferred into WT recipient mice and subsequently allowed to reach steady-state localization into the BM for a minimum of 4 h before administration of G-CSF or plerixafor and subsequent BM imaging was performed (Suratt et al., 2001; Fig. 3 b, experimental model 1). G-CSF treatment increased the motility of adoptively transferred GFP+ neutrophils in the skull BM with comparable efficacy to the effects previously observed with endogenous neutrophils in LysM-GFP mice (Fig. 3 c). Administration of G-CSF triggered the redistribution of GFP+ neutrophils toward BM sinusoids and promoted the release of these cells into the circulation (Fig. 3 d; Video 3). The release of GFP+ neutrophils from the BM peaked between 30 and 50 min after G-CSF administration (Fig. 3 e) and closely mirrored the increase in GFP+ neutrophils detected in the blood (Fig. 3 f). These findings indicate that neutrophil egress from the BM contributed to the number of circulating neutrophils in the blood of G-CSF–treated mice. In contrast, plerixafor treatment did not alter the motility of GFP+ BM neutrophils (Fig. 3 c). The rate of neutrophil egress from the BM in response to plerixafor was comparable to that observed at baseline (Fig. 3, d and e; Videos 4 and 5). However, plerixafor administration still led to a substantial increase of GFP+ neutrophils detected in the circulation (Fig. 3 f). These data suggest that although G-CSF stimulates neutrophil egress from the BM, the rapid increase in circulating neutrophils after CXCR4 inhibition by plerixafor treatment is largely independent of mobilization from this compartment.

CXCR4 does not play a direct active role in the mobilization of neutrophils

To further dissect out the contributions of CXCR2 and CXCR4 in neutrophil mobilization from the BM, we examined how transient inhibition of CXCR4 may influence KC-induced (KC, a CXCR2 ligand) neutrophil mobilization. As shown in Fig. 4 a, we observed that transient CXCR4 inhibition by plerixafor has a synergistic effect on KC-induced neutrophilia when a suboptimal dose of KC was administered. This synergistic effect by plerixafor diminished when higher concentrations were applied, indicating that CXCR2 is the dominant axis for neutrophil egress. Consistent with this
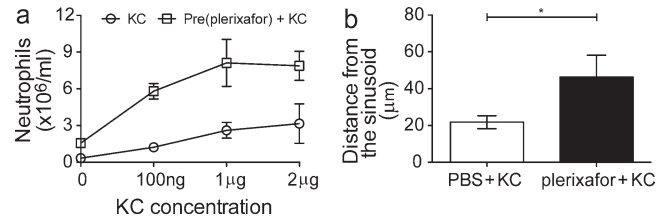

Figure 4. Role of CXCR2 and CXCR4 in KC–induced neutrophilia. (a) WT mice were pretreated for 1 h s.c. with plerixafor before i.v. treatment of KC at different doses. Number of circulating neutrophils detected 2 h after KC administration (n = 5 per group per dose). The control group consists of mice treated i.v. with KC only at specified doses. A representative set of data were shown from two independent experiments. All data are shown as mean ± SEM. (b) The mean traveling distance of neutrophils from the BM parenchyma to the sinusoids before egression. This was measured in LysM-GFP mice pretreated for 1 h with s.c. PBS or plerixafor after i.v. KC administration (500 ng per mouse). Graph shows dataset from a representative mouse (n = 3 per group). See also Video 6. All data are shown as mean ± SEM. A Student's two-tailed unpaired t test was performed. *, P < 0.05.

observation, our intravital imaging experiments also showed that plerixafor pretreatment augmented KC-induced neutrophil egress from the BM (unpublished data). We also observed that neutrophils which had eventually egressed from the BM were responding from distances further away from the sinusoids (Fig. 4 b and Video 6). Conceivably, blockade of the CXCR4 retention force allowed the neutrophils to become more responsive to KC stimulation. Together, our findings suggest that CXCR4 inhibition does not play a direct active role in neutrophil egress but instead lowers the threshold for mobilizing neutrophils from the BM.

Impaired neutrophil trafficking to the BM after plerixafor treatment increases circulating neutrophils

To visualize neutrophil trafficking to the BM, we infused freshly isolated LysM-GFP+ BM cells into WT recipient mice through the cannulated jugular vein 1 h after treatment with G-CSF or plerixafor (Fig. 5 a, experimental model 2). This approach allowed us to directly visualize the activities of GFP+ neutrophils from the time of first appearance in the microcirculation of the skull BM. In PBS-injected control mice and G-CSF–treated mice, the transferred GFP+ neutrophils were observed to adhere to the luminal surface of the BM sinusoidal walls as early as ~30 min after transfer, followed by transmigration into the BM parenchyma (Fig. 5 b and Video 7). Under these conditions, neutrophil transmigration into the BM compartment reached a plateau within ~2 h of cell transfer (unpublished data). In contrast, GFP+ neutrophil rolling along the vessel walls rarely resulted in recruitment into the BM parenchyma in plerixafor-treated mice (Fig. 5 b and Video 7). This result was confirmed by quantitative image analysis demonstrating a significant reduction in GFP+ neutrophils in BM parenchyma of plerixafor-treated animals compared with either G-CSF–treated mice or PBS-injected control animals (Fig. 5 c). The inhibition of GFP+ neutrophils trafficking
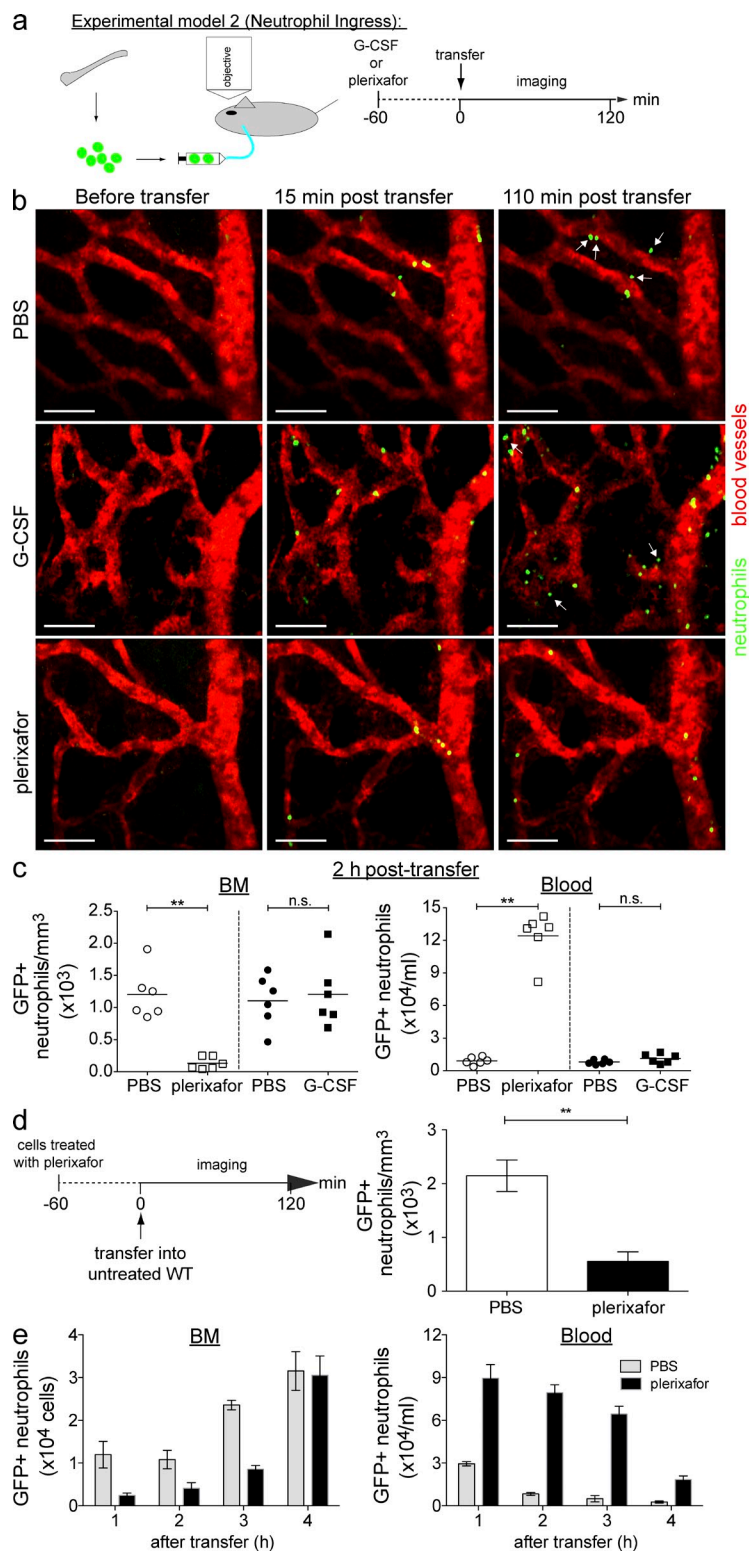
Figure 5. CXCR4 blockade inhibits neutrophil trafficking to the BM. (a) Experimental model 2: recipient WT mice were pretreated for 1 h s.c. with PBS, G-CSF, or plerixafor ($n = 6$ per group) before receiving BM cells from LysM-GFP mice via the cannulated jugular vein. (b) Representative time-lapse images showing neutrophil trafficking to the BM in PBS-treated mice (top), G-CSF–treated mice (middle) or plerixafor-treated mice (bottom). Arrows indicate GFP+ neutrophils (green) transmigrated from sinusoids (labeled with TRITC dextran; red) into the marrow space (black region). Bars, 40 µm. See also Video 7. (c, Left) Quantification of GFP+ neutrophils in skull BM cavity 2 h after treatment. (c, Right) Number of circulating GFP+ neutrophils 2 h after G-CSF or plerixafor treatment ($n = 6$ per group). Each symbol corresponds to one mouse and the bars represent mean GFP+ neutrophil numbers in each treatment group. (d, Left) The experimental procedure involved donor LysM-GFP mice pretreated for 1 h with s.c. PBS or plerixafor before transferring isolated treated BM cells into WT recipient mice via the cannulated jugular vein during imaging. (d, Right) Quantification of PBS-treated and plerixafor-treated GFP+ neutrophils in skull BM cavity 2 h after transfer ($n = 4$–5 per group). All data are shown as mean $\pm$ SEM. A Student's two-tailed unpaired t test was performed. **, $P < 0.01$; n.s. = not significant. (e) Recipient WT mice were pretreated for 1 h s.c. with PBS or plerixafor before receiving i.v. BM cells from LysM-GFP mice. 1–4 h after transfer of GFP+ BM cells, blood and perfused femur were collected and assessed via flow cytometry. (e, Left) The number of GFP+ neutrophils detected in the recipient BM. (e, Right) The number of circulating GFP+ neutrophils 1–4 h after transfer of BM cells ($n = 4$ per group per time point). A representative set of data were shown from two independent experiments. All data are shown as mean $\pm$ SEM.

to the BM in plerixafor–treated mice was accompanied by a reciprocal increase in circulating GFP+ neutrophil frequency (Fig. 5 c). To further understand if plerixafor acts directly on the neutrophils, we isolated LysM–GFP+ BM neutrophils from mice pretreated with plerixafor for 1 h before transferring these

treated cells into untreated recipient mice for subsequent imaging (Fig. 5 d). We observed that BM neutrophils from plerixafor-treated mice lacked the ability to traffic back to the BM at 2 h after transfer. This was further validated by flow cytometry experiments, whereby we observed that plerixafor-treated
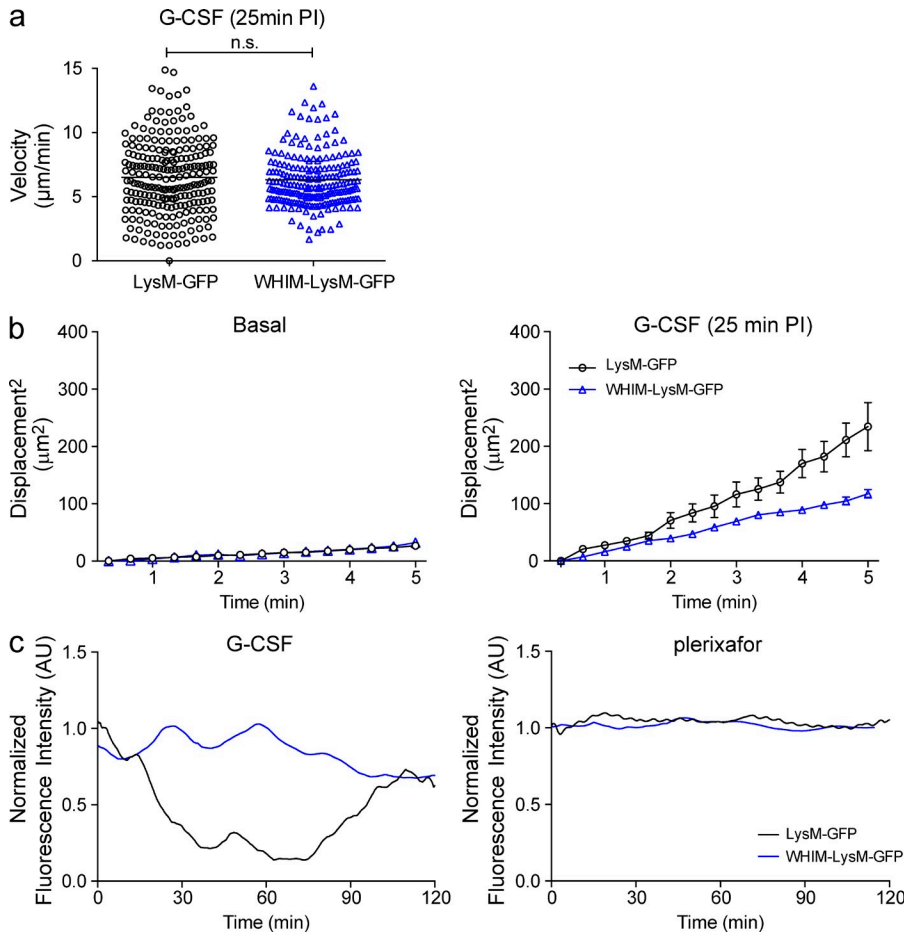
Figure 6. Neutrophil egress in LysM–GFP and WHIM–LysM–GFP mice. (a) Mean neutrophil migratory velocities at 25 min after G-CSF injection in skull BM of LysM-GFP and WHIM-LysM-GFP mice (5-min tracking period, n = 3 per group). Each symbol corresponds to an individual neutrophil tracked and the bars represent mean migratory velocity of each group. A Student's two-tailed unpaired t test was performed. n.s. = not significant. (b) Displacement of migrating GFP[+] neutrophils (relative to their initial positions) in LysM-GFP and WHIM-LysM-GFP mice during basal (left) and 25 min after G-CSF injection (right; 5-min tracking period, n = 3 per group). All data are shown as mean ± SEM. (c) Relative GFP fluorescence intensity in the skull BM parenchymal region in LysM-GFP and WHIM-LysM-GFP mice treated with G-CSF (left) or plerixafor (right) over time (representative of three independent experiments).

LysM–GFP[+] neutrophils were gradually detected in the BM over a period of 4 h that corresponds to a gradual reduction of these cells in the circulation (Fig. 5 e). Together, these data demonstrate that circulating neutrophil numbers can be increased dramatically by inhibiting homing of these cells to the BM.

Gain–of–function CXCR4 mutations altered neutrophil mobilization from the BM

To further understand the role of CXCR4 in neutrophil mobilization, we examined a CXCR4 gain-of-function genetic mouse model, i.e., an animal model for WHIM syndrome (Balabanian et al., 2012). For these experiments, we crossed the WHIM mouse onto LysM-GFP background to directly visualize how the gain-of-function mutations in CXCR4 may influence BM neutrophil activities and how plerixafor may act on these cells. We observed that although G-CSF was able to increase neutrophil motility in the BM of WHIM–LysM–GFP mice in a similar fashion as to the wild-type mice (Fig. 6 a), the mutant neutrophils displaced less as compared with their wild-type counterparts (Fig. 6 b). These results suggest that the CXCR4 gain-of-function mutation renders neutrophils less responsive to G-CSF–mediated egress signals. Consistent with this, quantification of the relative green fluorescent intensity in the BM also showed that the green fluorescent intensity remained relatively constant over the observation period,

indicating minimal neutrophil egress in response to G-CSF in the WHIM–LysM–GFP mice (Fig. 6 c). In addition, we also noted that plerixafor did not have an impact on neutrophil motility (not depicted) and egress in the WHIM–LysM–GFP mice (Fig. 6 c).

Plerixafor inhibits trafficking of CXCR4[mut] neutrophils to the BM in similar manner as to wild–type neutrophils

To better define the role of CXCR4 in the retention of neutrophils in the blood, we compared the mobilization ability of the CXCR4 gain-of-function neutrophils versus wild-type neutrophils using the ingress model established earlier (experimental model 2, see Fig. 3 a). This was performed by transferring a 1:1 ratio of selected Ly6G^{+} cells from the donor BM of both WHIM-LysM-GFP and WT-mT/mG mice into WT recipients pretreated for 1 h with PBS or plerixafor (Fig. 7 a). This method allowed us to easily detect and distinguish the two different fluorescent-tagged neutrophils in the recipient mice via flow cytometry. We observed that the circulating WHIM-LysM-GFP[+] neutrophil counts were significantly increased when mice were treated with plerixafor (Fig. 7 b). This increase in circulating neutrophils after plerixafor treatment was also observed with the WT-mT/mG[+] neutrophils. In contrast, in the BM of plerixafor-treated mice, we detected a significant reduction of both WHIM-LysM-GFP[+] and WT-mT/mG[+]

neutrophils. Collectively, this set of data demonstrates that the CXCR4 mutant neutrophils respond similarly to wild-type neutrophils during plerixafor treatment by increasing their retention in blood while preventing neutrophils from trafficking back to the BM.

Neutrophils are released from the pulmonary circulation in response to plerixafor

Our data showed that release of neutrophils from the BM compartments does not have a major role in plerixafor-induced neutrophilia, pointing to the possibility of alternative neutrophil sources. The lungs accumulate a large pool of transit-delayed (marginated) neutrophils under normal physiological conditions (Doerschuk et al., 1987; Lien et al., 1987; Kuebler et al., 1994; Doyle et al., 1997; Kreisel et al., 2010) established by the differentially increased resistance of the pulmonary microvascular bed toward neutrophils. Under physiological state, when dynamic equilibrium is expected (i.e., neutrophil influx equals neutrophil efflux), the reservoir of excess retained neutrophils forms the lung marginated pool. The concentration of neutrophils present in the pulmonary microvascular bed is thought to be 20–60× higher than that present in the large systemic vessels (Lien et al., 1987; Hogg et al., 1994), and the lung has been estimated to hold up to 10–30% of total blood volume (Dock et al., 1961). Thus, the release of neutrophils from the marginated pool in the lung could reasonably be expected to exert a significant impact on circulating neutrophil numbers.

We therefore sought to determine whether G-CSF and plerixafor treatments were capable of triggering the release of marginated neutrophils from the lungs to reenter the circulation. To achieve this, we devised a tandem sampling method of obtaining both arterial blood (carotid) and venous blood (inferior vena cava) while preserving the ventilation and perfusion of the lungs in live mice (Fig. 8 a). This approach allowed us to perform differential counts of neutrophils in arterial blood (exiting the lung) and venous blood (entering the lung) while avoiding the potential influence of interposing organs on neutrophil numbers. To validate our tandem sampling method, we used epinephrine as a positive control, which is known to induce rapid demargination of neutrophils from the lungs (Bierman et al., 1952b). This set of experiments showed that indeed, epinephrine treatment increases neutrophil release from the lungs (Fig. 8 b).

In plerixafor-treated mice, neutrophil frequency was significantly increased in arterial blood compared with venous blood, which peaked between 2 and 4 h after treatment and returned to basal level after 6 h. In contrast, G-CSF only had an effect on marginated neutrophils in the lung at a later time point (Fig. 8 c), and it is conceivable that the mechanism of action is through the down-regulation of CXCR4 expression (Kim et al., 2006). Indeed, we observed that after G-CSF treatment, neutrophils down-regulate CXCR4 expression gradually (unpublished data).

In addition, we have also determined the expression of CXCR4 ligand, CXCL12, in the lung using a CXCL12-GFP mice (Ara et al., 2003). By flow cytometry, we observed that CXCL12 is expressed by a fraction of endothelial cells, and with immunofluorescence staining of the lungs, we observed that CXCL12 is primarily expressed by capillary endothelial cells (Fig. 8 d). Collectively, these data indicate that the CXCR4–CXCL12 interactions contribute to the neutrophil margination and demargination process in the pulmonary circulation.

Having shown the increased release of neutrophils and expression of CXCL12, we next sought to visualize demargination of lung neutrophils in response to CXCR4 inhibition. We analyzed neutrophil activity in the subpleural capillaries of LysM-GFP mice using an intravital lung imaging model described recently (Looney et al., 2011; Fig. 8 e). Consistent with previous studies (Lien et al., 1987; Doyle et al., 1997; Kreisel et al., 2010; Looney et al., 2011), we observed a large number of marginated neutrophils within the pulmonary circulation under resting conditions. Administration of plerixafor triggered a reduction in the number of marginated neutrophils in the lungs within 2 h (Fig. 8 e). In contrast, the effects of G-CSF on marginated neutrophil numbers were negligible within this time frame, consistent with the neutrophil release data (Fig. 8 c and Video 8). As it is technically challenging to preserve the lungs under physiological conditions, each imaging field was imaged for
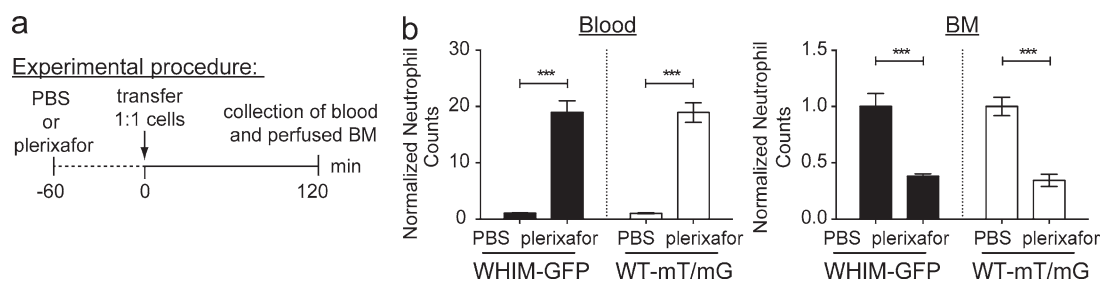

Figure 7. Neutrophil mobilization patterns of WHIM–LysM–GFP and WT–mT/mG mice. (a) The experimental procedure involved selection of Ly6G+ cells from BM cells isolated from donor WHIM-LysM-GFP and mT/mG mice. Cells were subsequently i.v. transferred in a 1:1 ratio into WT recipient mice pretreated for 1 h s.c. with PBS or plerixafor. 2 h after transfer of fluorescent-tagged cells, blood and perfused femur were collected. (b, Left) The normalized number of circulating fluorescent-tagged neutrophils 2 h after transfer. (b, Right) The normalized number of fluorescent-tagged neutrophils detected in the recipient BM (*n* = 4–5 per group). A representative set of data were shown from two independent experiments. All data are shown as mean ± SEM. Student's two-tailed unpaired *t* test was performed. ***, P < 0.001.
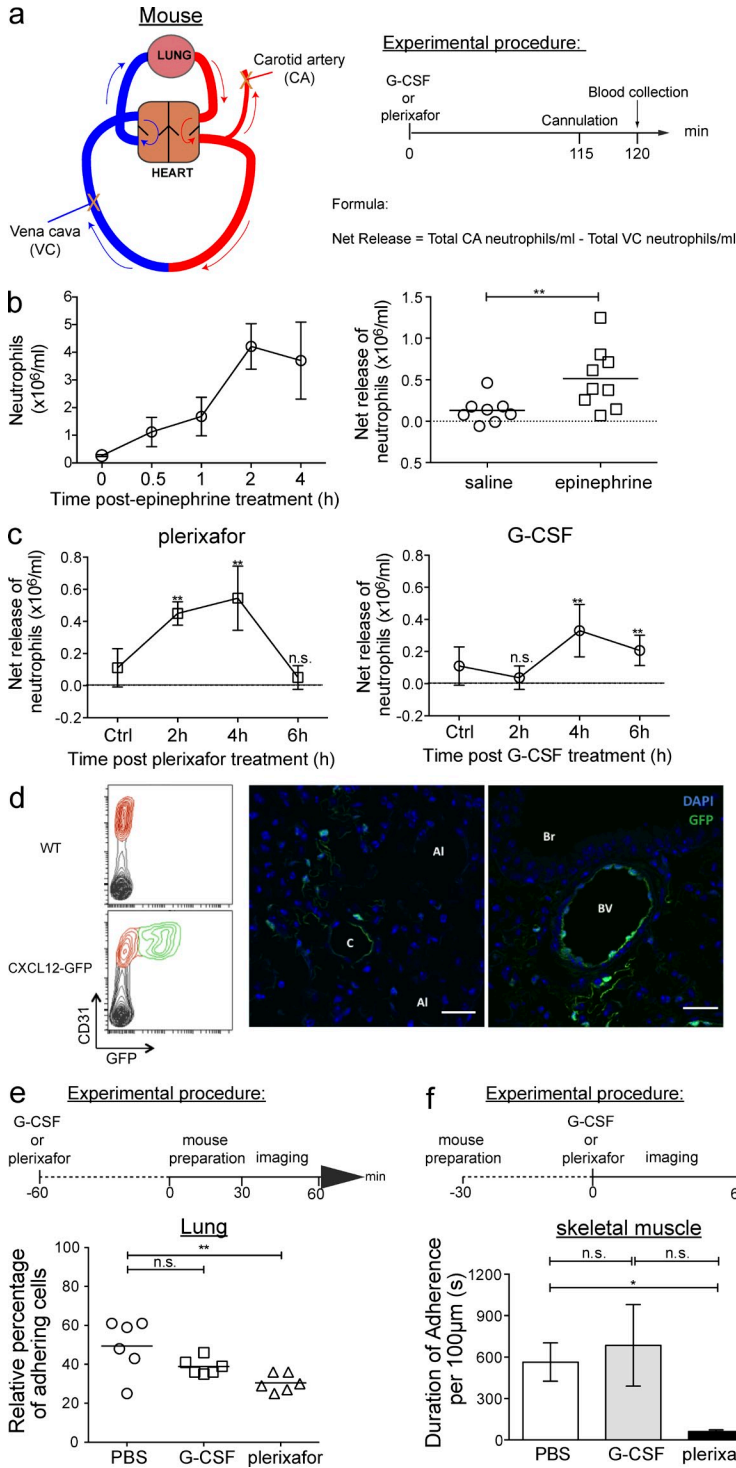
Figure 8. Plerixafor demarginates neutrophils from the lung through increase in net neutrophil release.
(a) A schematic representation of the simultaneous blood sampling method. Arrows indicate the direction of blood flow (blue = venous blood entering the lung; red = arterial blood exiting the lung). X indicates the carotid artery and inferior vena cava sites of blood collection. Mice received PBS, G-CSF, or plerixafor s.c., followed by the collection of blood samples from the cannulated carotid artery and vena cava 2 h after treatment (n = 5–7 per group per time point). Net neutrophil numbers released from lung were calculated using the formula indicated. (b, Left) Kinetics of circulating neutrophil numbers in WT mice in response to i.p. injection of 1 mg/kg epinephrine treatment (n = 4 mice per group per time point). All data are shown as mean ± SEM. (b, Right) Net neutrophil release from lungs 2 h after saline or epinephrine treatment. Each symbol corresponds to one mouse (n = 7–9 per group) and the bars represent mean neutrophil numbers in each treatment group. A Student's two-tailed unpaired t test was performed. **, P < 0.01. (c) Kinetics of net neutrophil release from lungs of mice treated s.c. plerixafor (left) or G-CSF (right; n = 6–8 per group per time point). Control group consists of mice treated s.c. with PBS. All data are shown as mean ± SEM. A Student's two-tailed unpaired t test was performed. **, P < 0.01; n.s. = not significant. (d, Left) A representative flow cytometry plot showing the endothelial marker, CD31, and GFP expression in lung cells of WT (top) and CXCL12-GFP (bottom) mice (n = 3 per group). (d, Right) Confocal images of lung sections from CXCL12-GFP demonstrating GFP expression in subpleural area (apical; left) and secondary bronchiole (middle, right). Images are representative of three independent experiments. Bars, 25 µm. C: capillary; AI: Alveoli; Br: Bronchiole; Bv: blood vessel. (e, Top) The experimental procedure for intravital imaging of the lung. Mice were pretreated for 90 min with PBS, G-CSF, or plerixafor s.c., followed by imaging using spinning-disk confocal microscopy. Five different fields from each lung were imaged for 5 min each. (e, Bottom) Quantification of neutrophils adhering to the pulmonary capillaries over the 5-min observation period in PBS-, G-CSF–, and plerixafor-treated mice (n = 6 per group). Each symbol corresponds to data obtained from an individual mouse and the bars represent the mean number of adherent neutrophils in each treatment group. See also Video 8. (f, Top) Experimental procedure for intravital multiphoton imaging of skeletal muscle involved preparation of the LysM-GFP mouse, followed by 1 h of imaging after s.c. injection of PBS, G-CSF, or plerixafor. (f, Bottom) The duration of neutrophil adherence measured in 100-µm lengths of muscle capillaries (3–6 capillaries, 4–7 µm in diameter) of LysM-GFP mice treated s.c. with PBS, G-CSF, or plerixafor (n = 3 per group). All data are shown as mean ± SEM. One-way ANOVA analysis was performed in e and f. *, P < 0.05; **, P < 0.01; n.s. = not significant. See also Video 9.

5 min and the data were presented as binary events. To further validate our data, we performed additional experiments to investigate neutrophil margination in the microcirculation of skeletal muscle in mice. This was done by measuring the overall dwell time of neutrophils along muscle capillaries (over the length of 100 µm). This approach allowed us to better examine the dynamic behavior of neutrophil margination in vivo, and we observed that plerixafor reduced neutrophil dwell time within the capillaries of muscle (Fig. 8 f and Video 9). This suggests that plerixafor–induced demargination could be a more generalized effect, which occurs throughout the entire vascular system, which may contribute to the rapid rise of neutrophil counts in the blood after plerixafor treatment.
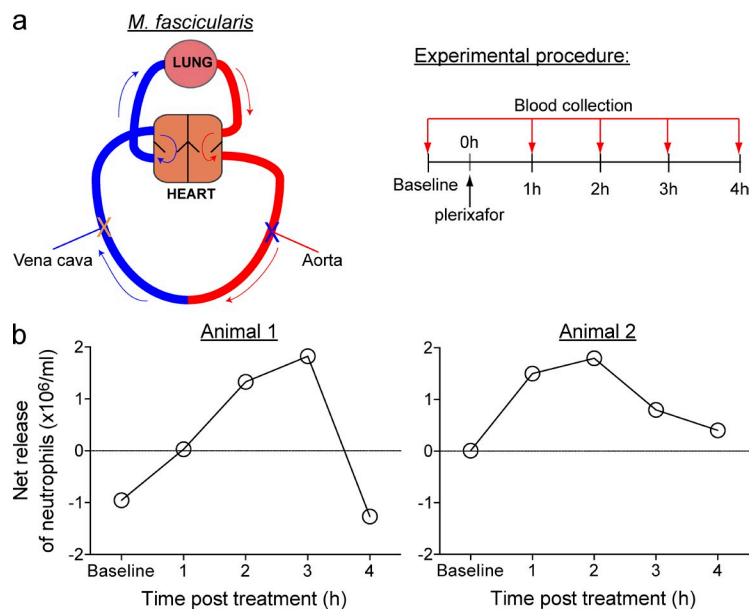
a

M. fascicularis

Experimental procedure:

Figure 9. Primate lung neutrophils are released after plerixafor treatment. (a, Left) A schematic representation of the simultaneous blood sampling method used in the nonhuman primate model *Macaca fascicularis*. Arrows indicate the direction of blood flow (blue = venous blood entering the lung; red = arterial blood exiting the lung). X indicates the aorta and inferior vena cava sites of blood collection. Blood was sampled from the aorta and vena cava before s.c. injection of 0.5 mg/kg plerixafor and then at 1-h intervals for a total duration of 4 h. (b) Net neutrophil release from the lungs of two individual animals over a 4-h observation period.

We finally sought to validate our plerixafor finding in a nonhuman primate model (*Macaca fascicularis*). Longitudinal collection of blood samples is not possible in mice; however, repeated sampling of blood from individual macaques permitted detailed assessment of the neutrophil counts over a 4-h period. 0.5 mg/kg plerixafor was administered s.c. to anesthetized animals and simultaneous blood sampling from the aorta and inferior vena cava was conducted every hour for 4 h thereafter (Fig. 9 a). Analogous to our earlier findings in mice, differential counting of neutrophil frequency in arterial and venous blood samples from two primates revealed an increased number of neutrophils in arterial blood after plerixafor treatment in both animals (Fig. 9 b). Neutrophil release from the lung peaked 2–3 h after plerixafor administration and returned to basal levels by 4 h.

Collectively, the findings from our study are the first to provide direct in vivo evidence demonstrating the ability of CXCR4 inhibition to induce demargination of neutrophils from the lung microvasculature and promote reentry of these cells into the circulation. These data supports the concept that the lung is an important source of neutrophils, which can be mobilized readily into the peripheral blood. Our demonstration that similar neutrophil demargination also occurs in nonhuman primates strongly suggests that our findings also extend to human patients.

DISCUSSION

Neutrophils are key mediators of host defense against microbial agents. The distribution of neutrophils between different tissue compartments is a tightly regulated process to maintain stable blood neutrophil counts at resting state, to allow rapid mobilization of neutrophils in response to inflammatory stimuli, and to return to a state of homeostasis after the immune response. Current prevailing views in the scientific community of how blood neutrophil counts are regulated are often rather simplistic; because the BM is the primary site of neutrophil production, any significant increases in circulating neutrophil numbers must therefore be attributed to their release from the BM. This overriding assumption has and may continue to lead to erroneous interpretations of end point studies such as those that relied on the quantification of neutrophil counts in the blood and/or BM as a readout. In the present study, we have used a combination of intravital imaging and in vivo homing assays to study the underlying cellular mechanisms of neutrophil mobilization in a highly compartmentalized manner. We observed that G-CSF and plerixafor work through two distinct cellular mechanisms affecting different compartments: G-CSF exerts its effects by increasing neutrophil mobilization and their release from the BM, which is in agreement with previous studies (Ulich et al., 1988; Semerad et al., 1999; Martin et al., 2003; Eash et al., 2010; Köhler et al., 2011b). However, contrary to the current paradigm, we found that inhibition of CXCR4 did not have a significant impact on BM neutrophil activities. Instead, plerixafor augmented the frequency of circulating neutrophils by simultaneously increasing the number of neutrophils reentering the circulation from the marginated pool present in the lung, as well as decreasing the number of neutrophils trafficking back to the BM, thereby increasing their retention in the blood.

It is well accepted that G-CSF–induced neutrophilia is a result of increased neutrophil release from the BM. This is established on the basis of G-CSF inducing an increase of neutrophils in the circulation, which is associated with a reciprocal decrease in the number of neutrophils in the BM (Ulich et al., 1988; Semerad et al., 2002; Martin et al., 2003). Indeed, data from our intravital imaging experiments showed that G-CSF increases BM neutrophil motility and redistribution of neutrophils around BM sinusoids, as also described by a recent study (Köhler et al., 2011b). Furthermore, G-CSF–induced neutrophil egress from the BM paralleled the appearance of additional

neutrophils in circulation, demonstrating that these cells are predominantly of BM origin. Of importance, our study has directly demonstrated for the first time that neutrophils that have trafficked back to the BM are able to maintain their capacity to reenter the circulation in response to G-CSF treatment. Thus, the BM may serve as a dynamic reservoir for storing and re-release of circulating neutrophils in response to fluctuating G-CSF levels, leading to implications in our understanding of the role of G-CSF in basic physiology, as G-CSF is produced in response to stress signals. Numerous prior studies have reported a role for CXCR4 in the retention of neutrophils in the BM (Martin et al., 2003; Eash et al., 2009; Petty et al., 2009; Eash et al., 2010). It has therefore been presumed that neutrophilia induced by CXCR4 blockade/plerixafor in both mice and human, results from increased neutrophil release from the BM (Martin et al., 2003; Dale et al., 2011; McDermott et al., 2011; Balabanian et al., 2012). However, there is little direct evidence that plerixafor can act as a BM neutrophil mobilizing agent in vivo. In fact, only a single ex vivo study of the perfused murine femoral BM has reported that plerixafor treatment can increase neutrophil release from this compartment (Martin et al., 2003). Because this study quantified neutrophils only in the femoral vein perfusate after plerixafor administration via the femoral artery, it was unclear whether the increase in neutrophil numbers observed in this model originated from the intravascular pool or the BM. In the current study, our in vivo imaging analyses revealed that plerixafor treatment did not exert a significant impact on BM neutrophil activity in either the endogenous or the cell transfer model. Despite exerting little effect on neutrophil mobilization from the BM, plerixafor still induced a substantial increase in circulating neutrophil numbers, indicating that CXCR4 inhibition may mobilize neutrophils to the blood from additional compartments other than the BM.

It has long been believed that the lung has the capacity to withdraw neutrophils from the blood into the pulmonary microvasculature and can deliver these cells back into the circulation when required (Bierman et al., 1952a). Indeed, neutrophils are rapidly released from the lung into the circulation within only seconds of epinephrine administration, indicating that the lung can serve as an important reservoir of these cells (Bierman et al., 1952b). Our own data revealed that CXCR4 inhibition triggers the release of neutrophils from the lung in both mice and nonhuman primates. The primate data are consistent with our intravital lung imaging data obtained in mice, which showed that fewer neutrophils are marginated in the lung after plerixafor treatment. Thus, in addition to its reported role in mediating the return of senescent neutrophils to the BM (Martin et al., 2003), our study identifies a novel role for CXCR4 in controlling neutrophil margination in the lung. It is tempting to speculate that the regulation of neutrophil removal from circulation by CXCR4 through the margination process is not restricted to the lung but represents a more generalized mechanism of blood neutrophil removal throughout the entire vascular system. This is supported by our findings that plerixafor also reduced neutrophil margination in the capillary beds of skeletal muscle. CXCL12 has been shown to activate integrins LFA-1 and VLA-4 on CD34+ human stem cells (Peled et al., 2000). Given that the integrins play a major role in cell adhesion, it is conceivable that CXCR4 regulates neutrophil margination in lungs by altering integrins expression, and this warrants further investigation. In addition, a previous study demonstrated that plerixafor treatment attenuates allergic lung inflammation (Lukacs et al., 2002). It is important for future studies to investigate the functional importance of CXCR4-mediated neutrophil margination/demargination in lungs, particularly to elucidate how this process may influence neutrophil recruitment into the lung in response to inflammation/infection, as this may have important implications for the clinical use of plerixafor.

Although our work focused extensively on G-CSF and plerixafor as therapeutic agents, if viewed from the perspective of G-CSF as a naturally occurring polypeptide factor and plerixafor as a CXCR4 signaling blocker, our mechanistic investigations have uncovered several startling conclusions about their physiological maintenance in dynamic equilibrium. This may have far-reaching consequences in how we traditionally perceive neutrophil and leukocyte homeostasis. Our current data suggests that the steady increase in neutrophil counts after G-CSF treatment could be mediated by distinct mechanisms that occur in different phases. In the early phase, mobilization of neutrophils from the BM acts as the main mechanism, but in the later phase, there is additional contribution from the demargination of neutrophils. Also, neutrophils in the BM become more responsive to mobilization signals in the later phase. It is important to point out that we are not contesting the value of data from previous works but highlighting that the short-term mechanistic action of the chemokine receptors are more complex and surprising than we would expect from long-term genetic studies. For instance, our cotransfer experiment showed that transient inhibition by plerixafor was able to alter WHIM neutrophil retention in blood and affect BM homing patterns in a similar fashion as wild-type neutrophils. Interestingly, during basal state, we observed a similar proportion of WHIM versus wild-type neutrophils that had trafficked back to the BM. This was unexpected, as prior studies had proposed the cause of abundance accumulation of mature neutrophils (myelokathexis) to be a result of increased neutrophil retention and homing to the BM (Balabanian et al., 2012). A possible explanation for this unexpected finding is the difference in the mechanisms regulating the process of neutrophil homing and egress in WHIM mice. It is conceivable that, under resting conditions, a gain-of-function in CXCR4 plays a functional dominant role in the chemotaxis and chemokinesis of neutrophils in the BM and a much lesser role in the chemotactic homing of neutrophils to the BM. This notion is supported by our imaging data which showed that despite G-CSF causing an increase in motility, WHIM neutrophil egress remained deficient and plerixafor treatment also had minimal effect on BM neutrophil egress. Thus, even in WHIM mice, the consequence of

increased circulating neutrophils with plerixafor treatment appears to be largely dependent on their decreased BM homing. To the best of our knowledge, our work is the first to demonstrate that constitutive CXCR4 signaling, as demonstrated in WHIM mice, promotes neutrophil retention in the BM (defective neutrophil egress) without affecting the efficiency of neutrophil homing (working neutrophil ingress), further highlighting the complexities of CXCR4 in these processes.

The concept of marginated pools as neutrophil reservoirs have been around for a long time, but this fundamentally important concept remains underappreciated. Our study is the first to demonstrate the crucial role of CXCR4–CXCL12 interactions in regulating the pulmonary marginated neutrophil pool, and that drastic change in the circulating neutrophil numbers can be achieved through mobilizing neutrophils from alternative reservoirs other than the BM, and hence demonstrates the importance of studying leukocyte homeostasis in an integrated manner that takes into consideration their compartmentalizations. Of interest, a previous study showed that CXCL12 can act as a vasoconstrictor and that this effect can be inhibited by plerixafor (Mieno et al., 2006). Thus, it is possible that plerixafor may induce changes in the cardiac output, which may be a contributing factor for the demargination of neutrophils in the lung.

From a clinical point of view, we have provided mechanistic insights into how G-CSF and plerixafor, despite their differing influences on neutrophil activity, consequently translate into increases in the number of circulating neutrophils. Our finding here with plerixafor also emphasizes that neutrophil mobilizing agents should be evaluated based on a comprehensive integrated approach, in which the neutrophil pool of different body compartments need to be considered holistically. Our current data shows that plerixafor treatment was able to induce neutrophil release from the lung up to 4 h after administration, and prevented neutrophils from homing back to the BM for up to 3 h. Despite the continued supply of circulating neutrophils from lung demargination, it was thus interesting to note that the overall circulating neutrophil numbers peaked at 1–2 h but returned to near basal levels by 4 h after plerixafor treatment. In contrast, we found that the rate of neutrophil trafficking back to the BM inversely correlated with neutrophil retention in the blood and was the stronger predictor of circulating neutrophil counts. Together, these results suggest that the plerixafor-induced neutrophil retention in the blood might be the primary mechanism responsible for the increased circulating neutrophil numbers detected, and that the demargination of neutrophils from the lung may play an important role only in the early stages after plerixafor treatment. Future studies should focus on examining whether plerixafor induces the presence of distinct populations of circulating neutrophils by changing their homing/margination patterns. Of particular interest, plerixafor is also used as a hematopoietic stem cell (HSC) mobilizing agent (Broxmeyer et al., 2005). In light of our current findings, it will be interesting to determine whether plerixafor-induced HSC mobilization derives solely from the BM. In conclusion, we believe that

evidence-based evaluation of drug action will facilitate the design of optimally tailored treatment regimens for neutrophil-related diseases. Further understanding of the biological function of the differential sources of neutrophils will be of particular importance for future studies as these neutrophils may possess distinct homing/adhesion pattern and/or cytokine secretion profile (Mantovani et al., 2011; Pillay et al., 2012).

METHODS AND MATERIALS

Mice. Mice 8–12 wk old were bred in the Biological Resource Centre (BRC) of A*STAR, Singapore, or in the University of Calgary animal facility and were maintained under specific pathogen-free conditions. LysM-GFP mice express enhanced GFP under the LysM promoter and were provided by T. Graf (Centre for Genomic Regulation, Barcelona, Spain; Faust et al., 2000). mT/mG mice (Muzumdar et al., 2007) and CX_3CR1 mice (Jung et al., 2000) were obtained from JAX mice. Gain-of-function CXCR4[mut] mice were generated as previously described (Balabanian et al., 2012). All mouse experiments were performed with the approval of the Institutional Animal Care and Use Committee of the BRC and the University of Calgary Animal Care Committee.

Neutrophil mobilizing reagents. Mice were injected s.c. with 250 µg/kg of recombinant human G-CSF (Roche; Semerad et al., 2002) or 5 mg/kg plerixafor (AMD 3100, Sigma-Aldrich; Broxmeyer et al., 2005; Eash et al., 2010). Control mice were injected s.c. with sterile PBS (Gibco). The dosages for G-CSF and plerixafor administered in mice had been optimized (Broxmeyer et al., 2005) to have comparable effects to doses administered in human clinical studies.

Generation of BM chimeras. Chimeric mice were generated via irradiation and BM transfer as described previously (Hoeffel et al., 2012). In brief, 6-wk-old mice were lethally irradiated with two doses of 550 rad spaced 3 h apart. BM cells were harvested from donor mice under sterile conditions and recipient mice were injected retro-orbitally with 5×10^6 BM cells within 24 h of irradiation. Recipient mice were maintained under SPF conditions for 8 wk before use in intravital multiphoton microscopy experiments.

Intravital multiphoton imaging of skull BM. Skull BM imaging was performed with minor modifications to published protocols (Mazo et al., 1998; Lo Celso et al., 2011). Mice were anaesthetized with a cocktail of 150 mg/kg ketamine and 10 mg/kg xylazine and immobilized on a custom-made stage. A heating pad affixed to the stage was used to maintain animal temperature at 37°C. A small area of skin on the skull was removed to expose the skull BM. The exposed skull was superfused with sterile PBS, covered with a glass coverslip, and visualized with a LaVision TriM Scope II microscope (LaVision BioTec), equipped with a 20× 1.4 NA WI objective lens and a Coherent Chameleon pulsed infrared laser. Experiments were performed at 880 nm excitation unless otherwise specified. Images were acquired using a 4-µm z-step size with an approximate z-depth of 50 µm. Image stacks were acquired every 20 s over a 2-h imaging period. To label blood vessels in vivo, mice were retro-orbitally injected with 4 mg TRITC-conjugated 155-kD dextran (Sigma-Aldrich) in 200 µl saline (Li et al., 2012). Imaging of the tibial BM was performed as previously described (Köhler et al., 2011a).

Image analysis. Images were transformed into time series movies and analyzed using IMARIS image analysis software (Bitplane). Tracking of cell motility in three dimensions was performed in a semiautomated manner as described previously (Ng et al., 2008, 2011). The mean/median and instantaneous migration velocities were typically obtained from 121 consecutive frames of video. To quantitate the endogenous neutrophil egress, the relative GFP fluorescence intensity was determined in specified regions of the marrow space using the surface function in surpass mode in IMARIS. For the analysis of experimental model 1 (neutrophil egress), the number of transmigrated GFP^{+} cells was quantified manually.

Murine BM cell isolation and transfer. The right femurs of LysM-GFP mice were removed and the femoral BM was harvested by flushing with ∼10 ml PBS containing 3% FCS. RBCs were lysed using commercial-grade RBC lysis buffer (eBioscience) and the remaining cells were resuspended in sterile PBS. In some experiments, 5×10^6 LysM-GFP$^+$ BM cells were delivered retro-orbitally or by catheterization and infusion via the left jugular vein. In another set of experiments, both the femur and tibia of WHIM-LysM-GFP and WT-mT/mG mice were removed and BM cells were harvested as described earlier. This was then followed by negatively selecting Ly6G$^+$ cells from BM cells with the EasySep mouse neutrophil enrichment kit (STEMCELL Technologies, Inc.). 2.5×10^6 neutrophils from WHIM-LysM-GFP$^+$ and WT-mT/mG$^+$ cells were subsequently mixed and delivered retro-orbitally.

Measurement of neutrophil numbers by flow cytometry. Cells isolated from the femur and/or blood was collected for analysis by flow cytometry. Samples were subjected to RBC lysis followed by incubation with blocking buffer (3% FCS and 5% rat serum in PBS) for 10 min. Cells were stained with the following antibodies: PE-conjugated CD115 (clone AFS98), PerCP-Cy5.5–conjugated CD11b (clone M1/70), and APC-Cy7–conjugated CD45 (clone 30-F11) from eBioscience; and APC-conjugated Ly-6G (clone 1A8) from BioLegend. Cells were stained with DAPI (Invitrogen) to assess cell viability and CountBright absolute counting beads (Invitrogen) were added before acquisition to enable calculation of absolute cell numbers. All samples were acquired using a FACSCanto II flow cytometer (BD) equipped with FACSDiva software. Data analysis was performed using FlowJo software (Tree Star).

Assessment of circulating neutrophils at different sites of blood collection. Mice were anaesthetized with a cocktail of 150 mg/kg ketamine and 10 mg/kg xylazine and placed on a heating pad at 37°C. The right carotid artery was cannulated using a previously described method (Duyverman et al., 2012). In brief, a midline incision was made on the neck and the glands were separated sideways to expose the trachea before the surrounding tissues were cleared to expose the underlying carotid artery. A polyethylene 10 tubing (inner diameter: 0.28 mm; outer diameter: 0.61 mm) was drawn to reduce the diameter at the tip for cannulation. A microvascular clamp was applied to the artery before insertion of the EDTA-filled tubing. The cannula was secured with a surgical suture and then the clamp was released to allow blood collection into an Eppendorf tube. Blood was then immediately withdrawn from the inferior vena cava using a 26G needle attached to a syringe prefilled with EDTA. Blood samples from different sites were prepared for FACS analysis as described earlier. In experiments using epinephrine as a positive control, epinephrine bitartrate salts (Sigma-Aldrich) were dissolved in saline and administered intraperitoneally at 1 mg/kg.

Flow cytometry analysis of CD31$^+$GFP$^+$ cells in lungs. Cells isolated from PBS-perfused lungs from wild-type and CXCL12-GFP mice were collected for analysis by flow cytometry. Lungs were harvested, minced, and incubated with 1 U/ml liberase (Roche) and 12 mU/ml DNase I (Sigma-Aldrich) in RPMI for 30 min at 37°C, pipetting every 5 min. Single cell suspensions were then stained with APC-conjugated and APC-Cy7–conjugated antibodies against CD31 and CD45. CD31$^+$GFP$^+$ cells were analyzed from the DAPI-negative and CD45-negative fraction.

Immunofluorescence analysis of CXCL12-GFP lungs. CXCL12-GFP mice were perfused with PBS followed by 2% paraformaldehyde. Lungs were harvested and placed in 2% paraformaldehyde overnight, followed by gradually preserving in 15 and 30% sucrose, before finally freezing in O.C.T. medium. 8-μm sections were hydrated in PBS for 10 min and mounted with Vectashield mounting media with DAPI. Images were acquired and analyzed with a confocal microscope (SPE; Leica) using LAS AF reprocessing software (Leica).

Spinning-disk confocal intravital imaging of lung. The detailed set-up for lung imaging can be found elsewhere (Looney et al., 2011). In brief, mice were anaesthetized with a cocktail of ketamine and xylazine and placed on a heater. Tracheostomy and catheterization of the jugular vein were performed surgically before the mice were connected to a mechanical ventilator (Mini Vent; HSE) and the lung exposed. To immobilize the lung, a custom-made vacuum window was positioned over the lung surface for the application of a negative pressure (40 mm Hg). The lung microvasculature was visualized at 10× magnification using a spinning-disk multichannel fluorescence intravital microscope (Quorum). Cell activity in the lung microvasculature was assessed using 488 and 635 nm lasers for excitation (typically 1-s duration) and then visualized using the appropriate long-pass filters (Semrock). A back-thinned electron–multiplying charge-coupled device camera (512 × 512 pixels; C9100-13; Hamamatsu) was used for fluorescence detection (Yipp et al., 2012). For delineation of the lung vasculature, mice were intravenously injected with 40 μg Alexa Fluor 647–conjugated bovine serum albumin (Invitrogen). Five different fields were recorded for 5 min and then analyzed to determine the total number of neutrophils per field. Neutrophils were defined as adherent if they remained stationary in the field for the entire imaging period. Data acquisition and analysis were performed using Volocity software (Perkin Elmer).

Intravital multiphoton imaging of skeletal muscle. The tibial anterior muscle was surgically prepared for imaging the skeletal muscle. LysM-GFP mice were anaesthetized with a cocktail of 150 mg/kg ketamine and 10 mg/kg xylazine. The left jugular vein was cannulated to allow the administration of 50 μg Evan's blue (Sigma-Aldrich) in 50 μl saline to label blood vessels in vivo. The mouse was subsequently immobilized on a custom-made stage and a heat pad was used to maintain the body temperature. To expose the skeletal muscle for imaging, a small area of skin was removed and loose dermal connective tissue was cleared to allow better visualization of the intact skeletal muscle vasculature. The exposed area was superfused with sterile PBS and sealed with a coverslip, with additional heating provided for the exposed muscle at 37°C. Experiments were performed at 950 nm excitation and images were acquired using a 5-μm z-step size with an approximate z-depth of 120 μm. Image stacks were acquired every 30 s over a 1-h imaging period.

Determination of circulating neutrophils in nonhuman primates. All experiments on adult female Macaca fascicularis nonhuman primates (2.5 kg and 3.2 kg, respectively) were performed at the SingHealth Experimental Medicine Centre (accredited by the Association for Assessment and Accreditation of Laboratory Animal Care) under approval #2012/SHS/692 from the Institutional Animal Care and Use Committee of Singapore. Mid-line laparotomy was performed under general anesthesia, and the retro-peritoneum was reflected along the mesenteric insertion. The descending abdominal aorta and inferior vena cava were identified and ∼1 ml blood was collected from each using a 25G needle 10 min before s.c. administration of 0.5 mg/kg plerixafor and at hourly intervals thereafter. Blood leukocyte counts were performed using a Hematology Analyzer (Beckman-Coulter).

Statistical analysis. Statistical analyses were conducted using Student's t test (normally distributed data) or one-way analysis of variance (ANOVA). P-values <0.05 were considered significant.

Online supplemental material. Fig. S1 shows assessment of leukocyte GFP expression in the BM of LysM-GFP mice. Video 1 shows neutrophil behavior in the skull BM. Video 2 shows dynamic behavior of neutrophil in the BM in response to G-CSF or plerixafor treatment. Video 3 shows that G-CSF increases neutrophil egress from the BM. Video 4 shows that plerixafor does not increase the number of neutrophil egress from the BM. Video 5 shows basal levels of neutrophil egress from the BM. Video 6 shows that plerixafor pretreatment augments KC-induced neutrophil egress from the BM. Video 7 shows neutrophil trafficking to the BM. Video 8 shows intravital imaging of neutrophils in the lung. Video 9 shows intravital imaging of neutrophils in skeletal muscle. Online supplemental material is available at http://www.jem.org/cgi/content/full/jem.20130056/DC1.

REFERENCES

Ara, T., K. Tokoyoda, T. Sugiyama, T. Egawa, K. Kawabata, and T. Nagasawa. 2003. Long-term hematopoietic stem cells require stromal cell-derived factor-1 for colonizing bone marrow during ontogeny. *Immunity*. 19:257–267. http://dx.doi.org/10.1016/S1074-7613(03)00201-2

Balabanian, K., E. Brotin, V. Biajoux, L. Bouchet-Delbos, E. Lainey, O. Fenneteau, D. Bonnet, L. Fiette, D. Emilie, and F. Bachelerie. 2012. Proper desensitization of CXCR4 is required for lymphocyte development and peripheral compartmentalization in mice. *Blood*. 119:5722–5730. http://dx.doi.org/10.1182/blood-2012-01-403378

Bierman, H.R., K.H. Kelly, F.L. Cordes, N.L. Petrakis, H. Kass, and E.L. Shpil. 1952a. The influence of respiratory movements upon the circulating leukocytes. *Blood*. 7:533–544.

Bierman, H.R., K.H. Kelly, F.L. Cordes, R.L. Byron Jr., J.A. Polhemus, and S. Rappoport. 1952b. The release of leukocytes and platelets from the pulmonary circulation by epinephrine. *Blood*. 7:683–692.

Broxmeyer, H.E., C.M. Orschell, D.W. Clapp, G. Hangoc, S. Cooper, P.A. Plett, W.C. Liles, X. Li, B. Graham-Evans, T.B. Campbell, et al. 2005. Rapid mobilization of murine and human hematopoietic stem and progenitor cells with AMD3100, a CXCR4 antagonist. *J. Exp. Med*. 201:1307–1318. http://dx.doi.org/10.1084/jem.20041385

Chtanova, T., M. Schaeffer, S.-J. Han, G.G. van Dooren, M. Nollmann, P. Herzmark, S.W. Chan, H. Satija, K. Camfield, H. Aaron, et al. 2008. Dynamics of neutrophil migration in lymph nodes during infection. *Immunity*. 29:487–496. http://dx.doi.org/10.1016/j.immuni.2008.07.012

Dale, D.C., A.A. Bolyard, M.L. Kelley, E.C. Westrup, V. Makaryan, A. Aprikyan, B. Wood, and F.J. Hsu. 2011. The CXCR4 antagonist plerixafor is a potential therapy for myelokathexis, WHIM syndrome. *Blood*. 118:4963–4966. http://dx.doi.org/10.1182/blood-2011-06-360586

Dock, D.S., W.L. Kraus, L.B. McGUIRE, J.W. Hyland, F.W. Haynes, and L. Dexter. 1961. The pulmonary blood volume in man. *J. Clin. Invest*. 40:317–328. http://dx.doi.org/10.1172/JCI104259

Doerschuk, C.M., M.F. Allard, B.A. Martin, A. MacKenzie, A.P. Autor, and J.C. Hogg. 1987. Marginated pool of neutrophils in rabbit lungs. *J. Appl. Physiol*. 63:1806–1815.

Doyle, N.A., S.D. Bhagwan, B.B. Meek, G.J. Kutkoski, D.A. Steeber, T.F. Tedder, and C.M. Doerschuk. 1997. Neutrophil margination, sequestration, and emigration in the lungs of L-selectin-deficient mice. *J. Clin. Invest*. 99:526–533. http://dx.doi.org/10.1172/JCI119189

Duyverman, A.M.M.J., M. Kohno, S. Roberge, D. Fukumura, D.G. Duda, and R.K. Jain. 2012. An isolated tumor perfusion model in mice. *Nat. Protoc*. 7:749–755. http://dx.doi.org/10.1038/nprot.2012.030

Eash, K.J., J.M. Means, D.W. White, and D.C. Link. 2009. CXCR4 is a key regulator of neutrophil release from the bone marrow under basal and stress granulopoiesis conditions. *Blood*. 113:4711–4719. http://dx.doi.org/10.1182/blood-2008-09-177287

Eash, K.J., A.M. Greenbaum, P.K. Gopalan, and D.C. Link. 2010. CXCR2 and CXCR4 antagonistically regulate neutrophil trafficking from murine bone marrow. *J. Clin. Invest*. 120:2423–2431. http://dx.doi.org/10.1172/JCI41649

Faust, N., F. Varas, L.M. Kelly, S. Heck, and T. Graf. 2000. Insertion of enhanced green fluorescent protein into the lysozyme gene creates mice with green fluorescent granulocytes and macrophages. *Blood*. 96:719–726.

Hernandez, P.A., R.J. Gorlin, J.N. Lukens, S. Taniuchi, J. Bohinjec, F. Francois, M.E. Klotman, and G.A. Diaz. 2003. Mutations in the chemokine receptor gene CXCR4 are associated with WHIM syndrome, a combined immunodeficiency disease. *Nat. Genet*. 34:70–74. http://dx.doi.org/10.1038/ng1149

Hoeffel, G., Y. Wang, M. Greter, P. See, P. Teo, B. Malleret, M. Leboeuf, D. Low, G. Oller, F. Almeida, et al. 2012. Adult Langerhans cells derive predominantly from embryonic fetal liver monocytes with a minor contribution of yolk sac-derived macrophages. *J. Exp. Med*. 209:1167–1181. http://dx.doi.org/10.1084/jem.20120340

Hogg, J.C., H.O. Coxson, M.L. Brumwell, N. Beyers, C.M. Doerschuk, W. MacNee, and B.R. Wiggs. 1994. Erythrocyte and polymorphonuclear cell transit time and concentration in human pulmonary capillaries. *J. Appl. Physiol*. 77:1795–1800.

Jung, S., J. Aliberti, P. Graemmel, M.J. Sunshine, G.W. Kreutzberg, A. Sher, and D.R. Littman. 2000. Analysis of fractalkine receptor CX(3)CR1 function by targeted deletion and green fluorescent protein reporter gene insertion. *Mol. Cell. Biol*. 20:4106–4114. http://dx.doi.org/10.1128/MCB.20.11.4106-4114.2000

Kim, H.K., M. De La Luz Sierra, C.K. Williams, A.V. Gulino, and G. Tosato. 2006. G-CSF down-regulation of CXCR4 expression identified as a mechanism for mobilization of myeloid cells. *Blood*. 108:812–820. http://dx.doi.org/10.1182/blood-2005-10-4162

Köhler, A., H. Geiger, and M. Gunzer. 2011a. Imaging hematopoietic stem cells in the marrow of long bones in vivo. *Methods Mol. Biol*. 750:215–224. http://dx.doi.org/10.1007/978-1-61779-145-1_15

Köhler, A., K. De Filippo, M. Hasenberg, C. van den Brandt, E. Nye, M.P. Hosking, T.E. Lane, L. Männ, R.M. Ransohoff, A.E. Hauser, et al. 2011b. G-CSF-mediated thrombopoietin release triggers neutrophil motility and mobilization from bone marrow via induction of Cxcr2 ligands. *Blood*. 117:4349–4357. http://dx.doi.org/10.1182/blood-2010-09-308387

Kreisel, D., R.G. Nava, W. Li, B.H. Zinselmeyer, B. Wang, J. Lai, R. Pless, A.E. Gelman, A.S. Krupnick, and M.J. Miller. 2010. In vivo two-photon imaging reveals monocyte-dependent neutrophil extravasation during pulmonary inflammation. *Proc. Natl. Acad. Sci. USA*. 107:18073–18078. http://dx.doi.org/10.1073/pnas.1008737107

Kuebler, W.M., G.E. Kuhnle, J. Groh, and A.E. Goetz. 1994. Leukocyte kinetics in pulmonary microcirculation: intravital fluorescence microscopic study. *J. Appl. Physiol*. 76:65–71.

Levesque, J.-P., F. Liu, P.J. Simmons, T. Betsuyaku, R.M. Senior, C. Pham, and D.C. Link. 2004. Characterization of hematopoietic progenitor mobilization in protease-deficient mice. *Blood*. 104:65–72. http://dx.doi.org/10.1182/blood-2003-05-1589

Li, J.L., C.C. Goh, J.L. Keeble, J.S. Qin, B. Roediger, R. Jain, Y. Wang, W.K. Chew, W. Weninger, and L.G. Ng. 2012. Intravital multiphoton imaging of immune responses in the mouse ear skin. *Nat. Protoc*. 7:221–234. http://dx.doi.org/10.1038/nprot.2011.438

Lien, D.C., W.W. Wagner Jr., R.L. Capen, C. Haslett, W.L. Hanson, S.E. Hofmeister, P.M. Henson, and G.S. Worthen. 1987. Physiological neutrophil sequestration in the lung: visual evidence for localization in capillaries. *J. Appl. Physiol*. 62:1236–1243.

Lieschke, G.J., and A.W. Burgess. 1992a. Granulocyte colony-stimulating factor and granulocyte-macrophage colony-stimulating factor (1). *N. Engl. J. Med*. 327:28–35. http://dx.doi.org/10.1056/NEJM199207023270106

Lieschke, G.J., and A.W. Burgess. 1992b. Granulocyte colony-stimulating factor and granulocyte-macrophage colony-stimulating factor (2). *N. Engl. J. Med*. 327:99–106. http://dx.doi.org/10.1056/NEJM199207093270207

Lo Celso, C., C.P. Lin, and D.T. Scadden. 2011. *In vivo* imaging of transplanted hematopoietic stem and progenitor cells in mouse calvarium bone marrow. *Nat. Protoc*. 6:1–14. http://dx.doi.org/10.1038/nprot.2010.168

Looney, M.R., E.E. Thornton, D. Sen, W.J. Lamm, R.W. Glenny, and M.F. Krummel. 2011. Stabilized imaging of immune surveillance in the mouse lung. *Nat. Methods*. 8:91–96. http://dx.doi.org/10.1038/nmeth.1543

Løvås, K., E. Knudsen, P.O. Iversen, and H.B. Benestad. 1996. Sequestration patterns of transfused rat neutrophilic granulocytes under normal and inflammatory conditions. *Eur. J. Haematol*. 56:221–229. http://dx.doi.org/10.1111/j.1600-0609.1996.tb01933.x

Lukacs, N.W., A. Berlin, D. Schols, R.T. Skerlj, and G.J. Bridger. 2002. AMD3100, a CxCR4 antagonist, attenuates allergic lung inflammation and airway hyperreactivity. *Am. J. Pathol*. 160:1353–1360. http://dx.doi.org/10.1016/S0002-9440(10)62562-X

Mantovani, A., M.A. Cassatella, C. Costantini, and S. Jaillon. 2011. Neutrophils in the activation and regulation of innate and adaptive immunity. *Nat. Rev. Immunol.* 11:519–531. http://dx.doi.org/10.1038/nri3024

Martin, C., P.C.E. Burdon, G. Bridger, J.C. Gutierrez-Ramos, T.J. Williams, and S.M. Rankin. 2003. Chemokines acting via CXCR2 and CXCR4 control the release of neutrophils from the bone marrow and their return following senescence. *Immunity*. 19:583–593. http://dx.doi.org/10.1016/S1074-7613(03)00263-2

Mazo, I.B., J.C. Gutierrez-Ramos, P.S. Frenette, R.O. Hynes, D.D. Wagner, and U.H. von Andrian. 1998. Hematopoietic progenitor cell rolling in bone marrow microvessels: parallel contributions by endothelial selectins and vascular cell adhesion molecule 1. *J. Exp. Med.* 188:465–474. http://dx.doi.org/10.1084/jem.188.3.465

McDermott, D.H., Q. Liu, J. Ulrick, N. Kwatemaa, S. Anaya-O'Brien, S.R. Penzak, J.O. Filho, D.A.L. Priel, C. Kelly, M. Garofalo, et al. 2011. The CXCR4 antagonist plerixafor corrects panleukopenia in patients with WHIM syndrome. *Blood*. 118:4957–4962. http://dx.doi.org/10.1182/blood-2011-07-368084

Mei, J., Y. Liu, N. Dai, C. Hoffmann, K.M. Hudock, P. Zhang, S.H. Guttentag, J.K. Kolls, P.M. Oliver, F.D. Bushman, and G.S. Worthen. 2012. Cxcr2 and Cxcl5 regulate the IL-17/G-CSF axis and neutrophil homeostasis in mice. *J. Clin. Invest.* 122:974–986. http://dx.doi.org/10.1172/JCI60588

Mieno, S., M. Boodhwani, B. Ramlawi, J. Li, J. Feng, C. Bianchi, R.J. Laham, J. Li, and F.W. Sellke. 2006. Human coronary microvascular effects of cardioplegia-induced stromal-derived factor-1alpha. *Ann. Thorac. Surg.* 82:657–663. http://dx.doi.org/10.1016/j.athoracsur.2006.03.044

Muzumdar, M.D., B. Tasic, K. Miyamichi, L. Li, and L. Luo. 2007. A global double-fluorescent Cre reporter mouse. *Genesis*. 45:593–605. http://dx.doi.org/10.1002/dvg.20335

Ng, L.G., A. Hsu, M.A. Mandell, B. Roediger, C. Hoeller, P. Mrass, A. Iparraguirre, L.L. Cavanagh, J.A. Triccas, S.M. Beverley, et al. 2008. Migratory dermal dendritic cells act as rapid sensors of protozoan parasites. *PLoS Pathog.* 4:e1000222. http://dx.doi.org/10.1371/journal.ppat.1000222

Ng, L.G., J.S. Qin, B. Roediger, Y. Wang, R. Jain, L.L. Cavanagh, A.L. Smith, C.A. Jones, M. de Veer, M.A. Grimbaldeston, et al. 2011. Visualizing the neutrophil response to sterile tissue injury in mouse dermis reveals a three-phase cascade of events. *J. Invest. Dermatol.* 131:2058–2068. http://dx.doi.org/10.1038/jid.2011.179

Peled, A., O. Kollet, T. Ponomaryov, I. Petit, S. Franitza, V. Grabovsky, M.M. Slav, A. Nagler, O. Lider, R. Alon, et al. 2000. The chemokine SDF-1 activates the integrins LFA-1, VLA-4, and VLA-5 on immature human CD34(+) cells: role in transendothelial/stromal migration and engraftment of NOD/SCID mice. *Blood*. 95:3289–3296.

Peters, N.C., J.G. Egen, N. Secundino, A. Debrabant, N. Kimblin, S. Kamhawi, P. Lawyer, M.P. Fay, R.N. Germain, and D. Sacks. 2008. In vivo imaging reveals an essential role for neutrophils in leishmaniasis transmitted by sand flies. *Science*. 321:970–974. http://dx.doi.org/10.1126/science.1159194

Petty, J.M., C.C. Lenox, D.J. Weiss, M.E. Poynter, and B.T. Suratt. 2009. Crosstalk between CXCR4/stromal derived factor-1 and VLA-4/VCAM-1 pathways regulates neutrophil retention in the bone marrow. *J. Immunol.* 182:604–612.

Pillay, J., V.M. Kamp, E. van Hoffen, T. Visser, T. Tak, J.-W. Lammers, L.H. Ulfman, L.P. Leenen, P. Pickkers, and L. Koenderman. 2012. A subset of neutrophils in human systemic inflammation inhibits T cell responses through Mac-1. *J. Clin. Invest.* 122:327–336. http://dx.doi.org/10.1172/JCI57990

Ponomaryov, T., A. Peled, I. Petit, R.S. Taichman, L. Habler, J. Sandbank, F. Arenzana-Seisdedos, A. Magerus, A. Caruz, N. Fujii, et al. 2000. Induction of the chemokine stromal-derived factor-1 following DNA damage improves human stem cell function. *J. Clin. Invest.* 106:1331–1339. http://dx.doi.org/10.1172/JCI10329

Semerad, C.L., J. Poursine-Laurent, F. Liu, and D.C. Link. 1999. A role for G-CSF receptor signaling in the regulation of hematopoietic cell function but not lineage commitment or differentiation. *Immunity*. 11:153–161. http://dx.doi.org/10.1016/S1074-7613(00)80090-4

Semerad, C.L., F. Liu, A.D. Gregory, K. Stumpf, and D.C. Link. 2002. G-CSF is an essential regulator of neutrophil trafficking from the bone marrow to the blood. *Immunity*. 17:413–423. http://dx.doi.org/10.1016/S1074-7613(02)00424-7

Shirozu, M., T. Nakano, J. Inazawa, K. Tashiro, H. Tada, T. Shinohara, and T. Honjo. 1995. Structure and chromosomal localization of the human stromal cell–derived factor 1 (SDF1) gene. *Genomics*. 28:495–500. http://dx.doi.org/10.1006/geno.1995.1180

Suratt, B.T., S.K. Young, J. Lieber, J.A. Nick, P.M. Henson, and G.S. Worthen. 2001. Neutrophil maturation and activation determine anatomic site of clearance from circulation. *Am. J. Physiol. Lung Cell. Mol. Physiol.* 281:L913–L921.

Suratt, B.T., J.M. Petty, S.K. Young, K.C. Malcolm, J.G. Lieber, J.A. Nick, J.-A. Gonzalo, P.M. Henson, and G.S. Worthen. 2004. Role of the CXCR4/SDF-1 chemokine axis in circulating neutrophil homeostasis. *Blood*. 104:565–571. http://dx.doi.org/10.1182/blood-2003-10-3638

Ulich, T.R., J. del Castillo, and L. Souza. 1988. Kinetics and mechanisms of recombinant human granulocyte-colony stimulating factor-induced neutrophilia. *Am. J. Pathol.* 133:630–638.

von Vietinghoff, S., and K. Ley. 2008. Homeostatic regulation of blood neutrophil counts. *J. Immunol.* 181:5183–5188.

Wengner, A.M., S.C. Pitchford, R.C. Furze, and S.M. Rankin. 2008. The coordinated action of G-CSF and ELR + CXC chemokines in neutrophil mobilization during acute inflammation. *Blood*. 111:42–49. http://dx.doi.org/10.1182/blood-2007-07-099648

Yipp, B.G., B. Petri, D. Salina, C.N. Jenne, B.N.V. Scott, L.D. Zbytnuik, K. Pittman, M. Asaduzzaman, K. Wu, H.C. Meijndert, et al. 2012. Infection-induced NETosis is a dynamic process involving neutrophil multitasking in vivo. *Nat. Med.* 18:1386–1393. http://dx.doi.org/10.1038/nm.2847